

NANO EXPRESS

Open Access



Properties of Longitudinal Electromagnetic Oscillations in Metals and Their Excitation at Planar and Spherical Surfaces

Vitaly V. Datsyuk* and Oleg R. Pavlyniuk

Abstract

The common definition of the spatially dispersive permittivity is revised. The response of the degenerate electron gas on an electric field satisfying the vector Helmholtz equation is found with a solution to the Boltzmann equation. The calculated longitudinal dielectric function coincides with that obtained by Klimontovich and Silin in 1952 and Lindhard in 1954. However, it depends on the square of the wavenumber, a parameter of the vector Helmholtz equation, but not the wave vector of a plane electromagnetic wave. This new concept simplifies simulation of the nonlocal effects, for example, with a generalized Lorents–Mie theory, since no Fourier transforms should be made. The Fresnel coefficients are generalized allowing for excitation of the longitudinal electromagnetic waves. To verify the theory, the extinction spectra for silver and gold nanometer-sized spheres are calculated. For these particles, the generalized Lorents–Mie theory gives the blue shift and broadening of the plasmon resonance which are in excellent agreement with experimental data. In addition, the nonlocal theory explains vanishing of the plasmon resonance observed for gold spheres with diameters less than or equal to 2 nm. The calculations using the Klimontovich–Silin–Lindhard and hydrodynamic dielectric functions for silver are found to give close results at photon energies from 3 to 4 eV. We show that the absolute values of the wavenumbers of the longitudinal waves in solids are much higher than those of the transverse waves.

Keywords: Nonlocal electrodynamics, Lindhard dielectric function, Surface plasmon resonance

Background

Irradiation of a plane metal surface by femtosecond laser pulses often results in formation of laser-induced periodic surface structures (LIPSSs) [1]. Besides the LIPSS, hyperfine ripples called high-spatial-frequency LIPSS (HSFL) were observed [1, 2]. The spatial periods of the HSFL are significantly smaller than the irradiation wavelength λ_0 . For example, for aluminum this period was estimated to range from 20 to 200 nm at $\lambda_0 = 0.8 \mu\text{m}$ [2, 3]. While orientation of the ripples in ordinary LIPSS was perpendicular to the laser light polarization, the orientation of HSFL was often perpendicular and sometimes parallel to the polarization. Similar HSFL were formed

on the surfaces of transparent dielectrics, semiconductors, and metals. The origin of the HSFL was explained by different mechanisms such as second-harmonic generation, the involvement of specific types of plasmon modes, self-organization, and local field enhancements during inhomogeneous breakdown in dielectric materials [2, 3].

The goal of this study is to search a wave process which could produce a pattern with a short period $\Lambda \ll \lambda_0$. We examine properties of longitudinal (L) electromagnetic waves in metals also known as plasma waves. Our study consists of the following novel steps. First, we started our research with definition of the spatial dispersion of the permittivity. As shown below, the common definition is useless if a medium under study is not uniform and infinite. Therefore, we propose a new concept of the spatially dispersive dielectric function ϵ . This function establishes the direct proportionality between two vector

*Correspondence: datsyuk@univ.kiev.ua
Department of Physics, Taras Shevchenko National University of Kyiv, 64,
Volodymyrska Str., 01601 Kyiv, Ukraine

fields, $\mathbf{E}(\mathbf{r}, \omega)$ and $\mathbf{D}(\mathbf{r}, \omega)$, but not the amplitudes $\mathbf{E}(\mathbf{k}, \omega)$ and $\mathbf{D}(\mathbf{k}, \omega)$ of plane waves. Consequently, the quantity ϵ depends on the square of the wave number, k^2 , the parameter of the vector Helmholtz equation for the electric field $\mathbf{E}(\mathbf{r}, \omega)$, but not the wave vector \mathbf{k} of the plane waves. Then, to derive such a novel function, we determined the response of the conduction electrons on an electromagnetic mode by solving the Boltzmann transport equation written in the relaxation-time approximation. The so-called transverse and longitudinal Lindhard dielectric functions were obtained. Further, we found that the longitudinal Lindhard and much simpler hydrodynamic function are close in a wide range of parameters. Light extinction by silver and gold nanospheres was considered in order to illustrate the theory. We show for the first time that the nonlocal Mie theory explains the blue shift, broadening, and eventual vanishing of the plasmon resonances observed with a decrease of the size of the noble-metal nanospheres. Finally, the newly developed theoretical model was applied to examine the possibility of involvement of the longitudinal modes in formation of the laser-induced surface structures. For this purpose, we modified the Fresnel theory taking into account transmitted longitudinal waves.

Methods

To determine the electromagnetic fields in piecewise homogeneous media, the classical electromagnetic theory was applied. The electric field \mathbf{E} in each uniform domain of the heterogeneous medium was assumed to be a solution of the vector Helmholtz equation (VHE):

$$\Delta \mathbf{E} + k^2 \mathbf{E} = 0, \quad (1)$$

where Δ is the Laplace operator.

As usual, the tangential components of the electric \mathbf{E} and magnetic \mathbf{H} fields are continuous across the boundaries of the media. In addition, we took into account that electrons are confined in metal; therefore, the following additional boundary condition (ABC) for the normal component of the current density \mathbf{j} at the metal surface S was used: $(\mathbf{j} \cdot \mathbf{n})|_{r \in S} = 0$.

To determine the conduction current in metal, we solved the Boltzmann transport equation (BTE) written in the relaxation time approximation:

$$\frac{\partial f}{\partial t} + \mathbf{v} \frac{\partial f}{\partial \mathbf{r}} + \frac{e}{m} (\mathbf{E} + \mathbf{v} \times \mathbf{B}) \frac{\partial f}{\partial \mathbf{v}} = \frac{f_0 - f}{\tau}, \quad (2)$$

where f is the single-particle distribution function in the phase space (\mathbf{r}, \mathbf{v}) , \mathbf{v} is the microscopic electron velocity, e and m are the electron charge and mass respectively, \mathbf{B} is the magnetic induction, f_0 is an equilibrium distribution function, and τ is the relaxation time.

Below, we derive formulas for the spatially dispersive dielectric functions. Then, we use them to study light

reflection from a plane metal surface and scattering of light on a noble-metal nanosphere.

Results and Discussion

Spatial Dispersion of ϵ in a Heterogeneous Medium

In the literature, a spatially dispersive dielectric function ϵ is defined via the following relation [4–6]:

$$\mathbf{D}(\omega, \mathbf{r}) = \epsilon_0 \iiint_{-\infty}^{\infty} d\mathbf{r}' \epsilon(\omega, \mathbf{r} - \mathbf{r}') \mathbf{E}(\omega, \mathbf{r}'), \quad (3)$$

where ϵ_0 is the electric constant, $\mathbf{D}(\omega, \mathbf{r})$ is the amplitude of the displacement vector oscillation with angular frequency ω in point \mathbf{r} , and $\mathbf{E}(\omega, \mathbf{r}')$ the amplitude of the electric-field oscillation in point \mathbf{r}' . Fourier transforms of Eq. (3) give the equation

$$\mathbf{D}(\omega, \mathbf{k}) = \epsilon_0 \epsilon(\omega, \mathbf{k}) \mathbf{E}(\omega, \mathbf{k}) \quad (4)$$

where a spatially dispersive $\epsilon(\omega, \mathbf{k})$ depends on the wave vector \mathbf{k} of a plane electromagnetic wave. In our opinion, Eq. (3) is not ambiguous only in an infinite homogeneous volume but we deal with piecewise heterogeneous system where boundaries should be taken into account and \mathbf{k} are not the same in different media.

Our approach does not use expansion of the electromagnetic waves over plane waves. The spatially dispersive permittivity determines the relation between $\mathbf{D}(\omega, \mathbf{r})$ and a particular solution to the vector Helmholtz Eq. (1):

$$\mathbf{D}(\omega, \mathbf{r}) = \epsilon_0 \epsilon(\omega, k) \mathbf{E}(\omega, \mathbf{r}). \quad (5)$$

Here $\mathbf{E}(\omega, \mathbf{r})$ denotes distribution of the electric field but not merely the vector \mathbf{E} in point \mathbf{r} .

Longitudinal and Transverse Dielectric Functions

The permittivity of metals is commonly expressed through the conductivity σ [4]:

$$\epsilon = \epsilon_g + \frac{i\sigma}{\omega \epsilon_0}, \quad (6)$$

where ϵ_g is a part of the dielectric function allowing for polarization of the solid; $\epsilon_g = 1$ for a simple metal. In order to determine σ , we calculated the current density

$$\mathbf{j} = e \iiint_{-\infty}^{\infty} \mathbf{v} f d\mathbf{v} = \sigma \mathbf{E}, \quad (7)$$

where $d\mathbf{v} = \frac{v}{m} d\epsilon d\Omega$, $d\Omega = \sin\theta d\theta d\phi$, v, θ, ϕ are the spherical coordinates of the velocity. Unlike previous researches, we did not introduce the wave vector \mathbf{k} but found a BTE solution in a form of an infinite series containing operators $\mathbf{v} \nabla$ acting on $\mathbf{v} \mathbf{E}$:

$$f = f_0 + \frac{e}{-i\omega + \Gamma} \frac{\partial f_0}{\partial \epsilon} \left[1 + \frac{\mathbf{v} \nabla}{-i\omega + \Gamma} \right]^{-1} \mathbf{v} \mathbf{E}, \quad (8)$$

where $\Gamma = 1/\tau$. Then, f_0 was approximated by a zero-temperature Fermi-Dirac distribution and, after integration over ϵ in Eq. (7), we got

$$\mathbf{j} = \frac{\omega_p^2 \epsilon_0}{-i\omega + \Gamma} \frac{3}{4\pi} \iint \mathbf{u} (1 + l\mathbf{u}\nabla)^{-1} (\mathbf{u}\mathbf{E}) d\Omega, \quad (9)$$

where $\omega_p^2 = \frac{e^2 n_e}{m \epsilon_0}$, ω_p is the plasma frequency, $\mathbf{u} = \frac{\mathbf{v}}{v}$ is the unit vector in the direction of \mathbf{v} , $l = \frac{v_F}{-i\omega + \Gamma}$, v_F is the Fermi velocity. Further, we calculated the integrals

$$\iint \mathbf{u} (\mathbf{u}\mathbf{E}) d\Omega = \frac{4\pi}{3} \mathbf{E} \quad (10)$$

$$\iint \mathbf{u} (\mathbf{u}\nabla)^{2n-1} (\mathbf{u}\mathbf{E}) d\Omega = 0 \quad (11)$$

$$\begin{aligned} \iint \mathbf{u} (\mathbf{u}\nabla)^{2n} (\mathbf{u}\mathbf{E}) d\Omega &= \frac{4\pi}{2n+3} \\ &\times \Delta^{n-1} \left[\nabla (\nabla \cdot \mathbf{E}) - \frac{1}{2n+1} \nabla \times \nabla \times \mathbf{E} \right] \end{aligned} \quad (12)$$

where n is a natural number. The following dependence of \mathbf{j} on an arbitrary electric field \mathbf{E} was finally obtained

$$\begin{aligned} \mathbf{j} &= \frac{\omega_p^2 \epsilon_0}{-i\omega + \Gamma} \left\{ \mathbf{E} + 3 \sum_{n=1}^{\infty} l^{2n} \right. \\ &\times \left. \frac{\Delta^{n-1}}{2n+3} \left[\nabla (\nabla \cdot \mathbf{E}) - \frac{\nabla \times \nabla \times \mathbf{E}}{2n+1} \right] \right\}. \end{aligned} \quad (13)$$

There are two types of solutions to Eq. (1), divergence-free which satisfy equation $\nabla \cdot \mathbf{E} = 0$ and rotationless which satisfy equation

$$\nabla \times \mathbf{E} = 0. \quad (14)$$

For a plane wave, with $E \propto \exp[i(\mathbf{k}\mathbf{r} - \omega t)]$, Eq. (14) transforms into the relation $\mathbf{k} \times \mathbf{E} = 0$ which shows that the wave is longitudinal (L). To simulate processes in spherical bodies, it is convenient to use the vector spherical harmonics \mathbf{L} , \mathbf{M} , and \mathbf{N} as a complete set of orthogonal functions. In this case, Eq. (14) specifies harmonics \mathbf{L} . The wavenumber of the L waves and \mathbf{L} modes is determined by the following dispersion law

$$\epsilon^L(\omega, k^L) = 0. \quad (15)$$

From Eqs. (6) and (13) we find that solutions to Eq. (1) satisfying the constraint of Eq. (14) give the following longitudinal permittivity

$$\epsilon^L = \epsilon_g - \frac{\omega_p^2}{\omega(\omega + i\Gamma)} \frac{3}{2} \Phi\left(a^2, 1, \frac{3}{2}\right) \quad (16)$$

where Φ is the Lerch's Phi function,

$$\frac{3}{2} \Phi\left(a^2, 1, \frac{3}{2}\right) = \sum_{n=0}^{\infty} \frac{3}{2n+3} a^{2n}, \quad (17)$$

$$a = \frac{kv_F}{\omega + i\Gamma}.$$

The obtained permittivity differs from that defined by Kliewer and Fuchs [7] only in notation:

$$\epsilon^L = \epsilon_g + \frac{\omega_p^2}{\omega(\omega + i\Gamma)} \frac{3}{a^2} \left[1 - \frac{1}{ia} \tan^{-1}(ia) \right] \quad (18)$$

The identity

$$\frac{1}{ia} \tan^{-1}(ia) = \frac{1}{2} \ln \frac{1+a}{1-a} \quad (19)$$

allows one to rewrite Eq. (18) as follows

$$\epsilon^L = \epsilon_g - \frac{\omega_p^2}{\omega(\omega + i\Gamma)} \frac{3}{a^2} \left[1 - \frac{1}{2a} \frac{\ln(1+a)}{\ln(1-a)} \right]. \quad (20)$$

In the case of $\Gamma = 0$, this formula takes the form of an equation derived by Klimontovich and Silin [8] who studied Landau dumping in degenerate plasma (see [9], [10, Eq. (40.17)], and [11]). The permittivity of the equivalent Eqs. (16), (18), and (20) is commonly called the Lindhard dielectric function (with reference to [12]) though this function was first obtained by Klimontovich and Silin [8].

The transverse Lindhard permittivity [7] can be found with Eq. (13) when $\nabla \cdot \mathbf{E} = 0$. In the actual case of $v_F k \ll \omega$, it reduces to the Drude dielectric function

$$\epsilon^T = \epsilon_g - \frac{\omega_p^2}{\omega^2 + i\Gamma\omega}. \quad (21)$$

This function agrees with experimental data on many metals [13]. If $|a| < 1$, the longitudinal permittivity (16) simplifies to the hydrodynamic dielectric function:

$$\epsilon^L(\omega, k^L) = \epsilon_g - \frac{\omega_p^2}{\omega^2 + i\Gamma\omega - \frac{3}{5}(v_F k^L)^2}. \quad (22)$$

Reflection of a Plane Electromagnetic Wave from a Flat Metal Surface

Boundary Conditions

In this section, we determine the direction of the wave vector k^L and amplitude of the L wave excited in metal during reflection of a plane electromagnetic wave from a flat metal surface.

Consider plane wave incident on the dielectric-metal interface $z = 0$ with the wave vector lying in the xz plane. The electric field in the dielectric medium 1 consists of the incident \mathbf{E}_i and reflected \mathbf{E}_r waves, the field in metal 2 has the transmitted transverse \mathbf{E}_t and, in some cases, longitudinal \mathbf{E}^L components. According to the Maxwell boundary conditions, the transverse components of the electric and magnetic field vectors are continuous in plane $z = 0$. In addition, the electrons are not ejected from metal; therefore, the normal component of the electric current density is zero at $z = 0$,

$$\hat{\mathbf{z}} \mathbf{j}|_{z=0} = 0. \quad (23)$$

where $\hat{\mathbf{z}}$ is the unit vector in the direction of z axis.

All terms in the Maxwell boundary conditions must have the same dependence on x and y . This requirement has several consequences. First, it can be established that L waves can be excited only in the case of p-polarization when the electric vector of the incident wave $\mathbf{E}^{(i)}$ is parallel to the plane of incidence. In other words, plasmon polaritons can be generated by a transverse magnetic (TM) wave. The effect is much the same as in a metal sphere [14]. Secondly, formulas akin to the Snell's law can be derived from the conditions

$$k_{1x} = k_{2x} = k_{2x}^L = k_1 \sin \theta_1 \quad (24)$$

where indexes $1x$ and $2x$ denote the x -projections of the vectors in media 1 and 2, respectively, θ_1 is the angle of incidence.

Reflection and Transmission Coefficients

Let us determine the field formed by a plane p-polarized electromagnetic wave incident on a plane metal surface. It is convenient to express the components of the electric and magnetic fields through the x component of $\mathbf{E}^{(i)}$, namely $E_x^{(r)} = -r E_x^{(i)}$ for the reflected wave, $E_x^{(t)} = t E_x^{(i)}$ for the transmitted transverse wave, and

$$E_x^{(a)} = \delta E_x^{(t)} = t_L E_x^{(i)} \quad (25)$$

for the transmitted longitudinal wave, here r is a reflection coefficient, t and t_L are transmission coefficients.

From the Maxwell boundary conditions and ABC of Eq. (23) written in the following form

$$\hat{\mathbf{z}} \cdot (\mathbf{D} - \epsilon_0 \epsilon_g \mathbf{E})|_{z=0} = 0, \quad (26)$$

we got

$$r = -\frac{(1 + \delta) \epsilon_1 k_{2z} - \epsilon_2 k_{1z}}{(1 + \delta) \epsilon_1 k_{2z} + \epsilon_2 k_{1z}} = 1 - (1 + \delta) t \quad (27)$$

$$t = \frac{2 \epsilon_1 k_{2z}}{\epsilon_2 k_{1z} + (1 + \delta) \epsilon_1 k_{2z}}, \quad (28)$$

$$\delta = \frac{\epsilon_g - \epsilon}{\epsilon_g} \frac{k_{2x}^2}{k_{2z} k_{2z}^L} \quad (29)$$

At $\delta = 0$, the coefficient r becomes the Fresnel coefficient of reflection of the p-polarized wave (see, for instance, Eq. (2.49) of [4]). Under the same condition, t is not the Fresnel transmission coefficient since our definitions of t and r differ from the Fresnel's ones.

Extinction of Light by Metal Nanosphere

In a preceding paper, one of the authors generalized the Lorentz-Mie theory allowing for the ABC of Eq. (23). An analog of the Fresnel coefficient r , the Mie coefficient

b_l for the reflected TM mode of the l th order was found to be

$$b_l = -\frac{(1 + \delta_l) \epsilon_1 \frac{k_2 \psi_l'(k_2 R)}{\psi_l(k_2 R)} - \epsilon_2 \frac{k_1 \psi_l'(k_1 R)}{\psi_l(k_1 R)}}{(1 + \delta_l) \epsilon_1 \frac{k_2 \psi_l'(k_2 R)}{\psi_l(k_2 R)} - \epsilon_2 \frac{k_1 \zeta_l'(k_1 R)}{\zeta_l(k_1 R)}}, \quad (30)$$

where

$$\delta_l = \frac{\epsilon^T - \epsilon_g}{\epsilon_g} \frac{l(l+1) j_l(k_2 R) j_l(k_2^L R)}{\psi_l'(k_2 R) k_2^L R j_l'(k_2^L R)}, \quad (31)$$

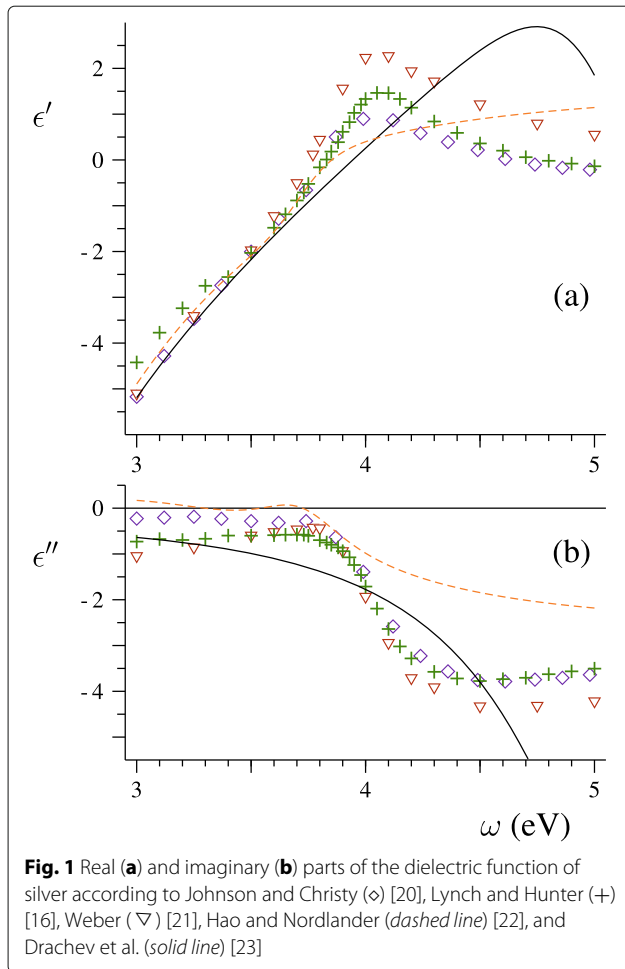
ψ_l and ζ_l are the Riccati-Bessel and Riccati-Hankel functions of the order l , respectively; j_l is the spherical Bessel function, the prime denotes the derivative of a function with respect to its argument.

Let us compare predictions of the classical and generalized Lorentz-Mie theories with experimental data. In [15], Hilger, Tenfelde, and Kreibig studied extinction spectra of silver nanoparticles deposited on dielectric surfaces. In the first stage of the study, the researchers generated beams of silver particles with mean diameters of 2, 3.5, and 4 nm, determined the particle size distribution for one of the beams, recorded extinction spectra, and estimated parameter $A = 0.25$ of the phenomenological formula $\Gamma = \Gamma_b + A \nu_F/R$, where Γ_b is the bulk-metal relaxation rate, for silver spheres in vacuum. First, we calculated the extinction spectra for a beam of silver spheres with the mean diameter $\langle D \rangle = 2$ nm and experimental size distribution which spans the region from $D = 1$ to $D = 4$ nm. Our theory contains no adjustable parameters. In order to define the dielectric functions, we used the tabulation of the refractive index of bulk silver proposed by Lynch and Hunter [16] (see Fig. 1). We also applied Eqs. (16), (21), and (22) with $\omega_p = 9.17$ eV, $\Gamma_b = 0.021$ eV, $\nu_F = 1.39 \times 10^6$ m/s, and $A = 0.25$. The results of the calculations and experimental spectrum are presented in Fig. 2.

The theoretical spectra in Fig. 2 were calculated using the Klimontovich-Silin-Lindhard and much simpler hydrodynamic dielectric functions. It is surprising that both calculations gave close results even though $|\alpha| > 1$ in the region of the plasmon resonance.

For the nanometer-sized silver spheres, the maximum in the extinction spectrum, called the Fröhlich [17], plasmon, and surface plasmon polariton (SPP) [15] resonance, is known to shift from 3.5 to 3.65 eV [18]. The nonlocal model is in excellent agreement with the experimental data, while the local (Mie) theory gives the maximum at $\omega \simeq 3.5$ eV (see Fig. 2 and Table 1).

The calculation of the blue shift of the plasmon resonance can be supported by the following consideration. In the electrostatic approximation, only b_1 contributes to the



extinction cross section Q_{ext} and Eq. (30) can be simplified by using the following approximations

$$\frac{k_2 R \psi'_l(k_2 R)}{\psi_l(k_2 R)} \simeq l + 1; \quad \frac{k_1 R \zeta'_l(k_1 R)}{\zeta_l(k_1 R)} \simeq -l. \quad (32)$$

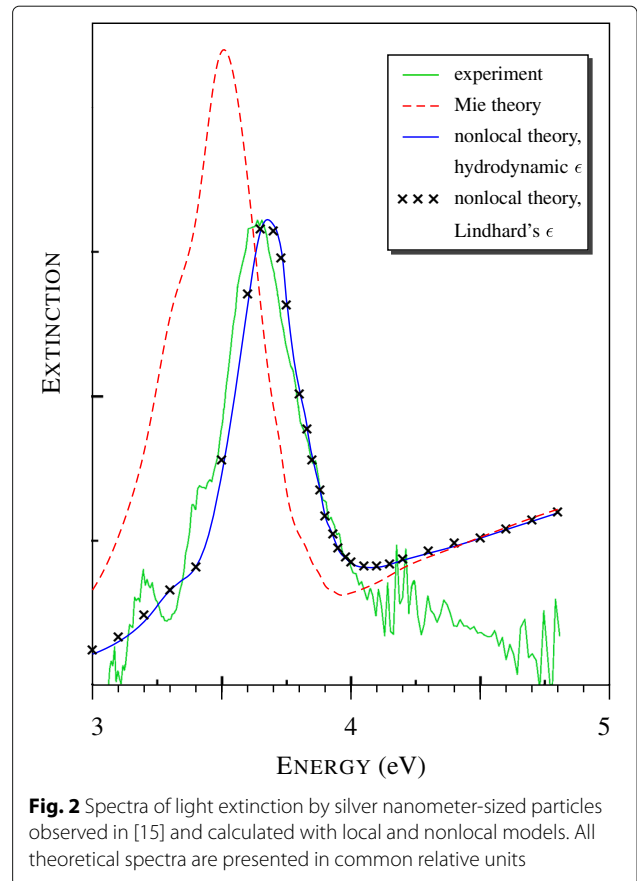
Thus, Q_{ext} has a maximum at

$$\Re[2(1 + \delta_1)\epsilon_1 + \epsilon_2] = 0. \quad (33)$$

The obtained condition (33) takes into account excitation of the L modes (by the term δ_1) and, therefore, differs from the Fröhlich resonance condition [17]:

$$\Re(2\epsilon_1 + \epsilon_2) = 0. \quad (34)$$

In experiment [15], the peak frequencies ω_m and resonance widths $\Delta\omega$ of the extinction spectra were almost independent of $\langle D \rangle$. This feature of $\Delta\omega$ seems to disagree with the classical Mie theory. Really, the local theory predicts broadening of the plasmon resonances with the decrease in D (at $A = 0.25$) as shown in Table 1. At the same time, the nonlocal theory gives approximately equal resonance widths but different peak positions. Superposition of the contributions from all particles gives the value



of $\Delta\omega$ which are in remarkable agreement with the experimental data. It is interesting that the nonlocal theory predicts a broadening of the plasmon resonance of a beam even at $A = 0$.

At $\omega > 4$ eV, the smooth theoretical curves in Fig. 2 lie higher than the mesh of narrow closely located experimental peaks. The interband absorption dominates in this spectral range as can be confirmed by Fig. 1. The observed peculiarities of the spectrum are likely to be a consequence of a transition from the continuum bands to a discrete level structure. Such a quantum-size effect was discovered earlier in a study of the optical properties of gold nanospheres [19]. When the silver-sphere size was increased to $\langle D \rangle = 3.5$ nm, the absorption first increased relative to the maximum and formed a plateau with a series of small equidistant dips. Then, the absorption slightly decreased at $\langle D \rangle = 4$ nm.

In order to study the formation of the blue wing of the plasmon resonance, we calculated the extinction spectra of ultra-tin silver particles and presented them in Fig. 3. A remarkable feature in Fig. 3 is complete vanishing of the plasmon resonance at $D = 1$ nm. Earlier, this effect was observed in the experimental study of gold nanospheres [19]. In particular, in Fig. 9 of [19], the experimental spectra of particles with diameters of 1.7, 1.9, 2.0, 2.1,

Table 1 Resonant frequencies and widths of the dipolar plasmon resonance of single silver particles and particles' beam

Size	ω_m (eV)				$\Delta\omega$ (eV)			
	THEORY							
	Local		Nonlocal		Local		Nonlocal	
	$A = 0$	$A = 0.25$	$A = 0$	$A = 0.25$	$A = 0$	$A = 0.25$	$A = 0$	$A = 0.25$
$D = 4$ nm	3.50	3.51	3.61	3.61	0.23	0.36	0.20	0.26
$D = 3$ nm	3.50	3.51	3.65	3.65	0.23	0.39	0.18	0.26
$D = 2$ nm	3.51	3.51	3.74	3.74	0.23	0.44	0.15	0.28
$D = 1$ nm	3.51	3.51	–	–	0.23	0.58	–	–
$\langle D \rangle = 2$ nm	3.50	3.51	3.68	3.68	0.23	0.42	0.25	0.33
	EXPERIMENT							
$\langle D \rangle = 2$ nm	3.65				0.33			

2.3, and 2.5 nanometers were compared with the spectra calculated with the local Mie theory. The agreement was poor, failing to describe the broadening of the plasmon resonance and its position [19]. The attempts to improve the fit by varying the size of the particles and modifications of the dielectric functions were not successive. According to the authors of [19], the observed abnormally wide or depressed collective oscillation band resists to be fitted with the proposed corrections of the local Mie theory. As can be seen from Fig. 4, the situation changes dramatically if the nonlocal Mie theory is applied. Note that we used no adjustable parameters. The tabulation of the complex refractive index by Johnson and Christy [20] was used to determine the dielectric function of gold. Other parameters, including $A = 1$ and refractive index of toluene (1.37) were taken from [19].

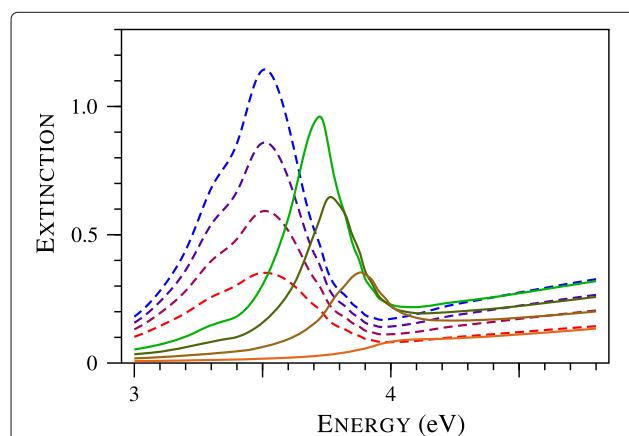


Fig. 3 Normalized extinction cross section of silver particles with diameters of 2.2, 1.8, 1.4, and 1.0 nm calculated with local (dashed lines) and nonlocal (solid curves) Mie theories. The smaller the particle, the lower the curve. All theoretical cross sections are presented in common relative units

Wave Numbers of the Longitudinal Waves

The longitudinal modes differ from the transverse ones by much higher values of the wavenumbers. For example, for the calculations presented in Fig. 2, the real part of k_2^L corresponds to the spatial period $\Lambda = 2\pi/\Re k_2^L$ decreasing from 9 to 2 nm at ω increasing from 3 to 4 eV. In this ω interval, the absolute value of the ratio k_2^L/k_2 decreased from 130 to 100 and the parameter δ of Eq. (27) decreased from 0.01 to 0.005 at $\theta_1 = \pi/4$. We conclude, therefore, that excitation of the L waves at a flat silver surface can be

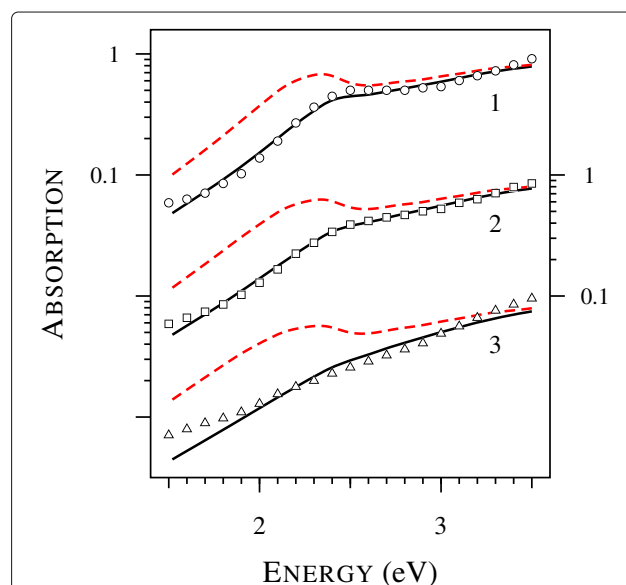


Fig. 4 Absorption spectra calculated with the local (dashed lines) and nonlocal (solid lines) Mie theory and experimental data (dots) extracted from Fig. 9 of [19] for gold spheres with $D = 2.5, 2.1,$ and 1.7 nm in toluene (curves 1 and circles, curves 2 and squares, and curves 3 and triangles, respectively). All theoretical spectra are normalized to unity at 4.12 eV and displaced vertically

neglected. However, the **L** modes have been found to be of importance in nanometer-sized silver clusters.

A replacement of the term $-\omega_p^2/(\omega^2 + i\Gamma\omega)$ in Eq. (16) by $\epsilon^T - \epsilon_g$ according to Eq. (21) allows us to rewrite the dispersion Eq. (15) in the following form

$$1 + \frac{3}{5}a^2 + \frac{3}{7}a^4 + \frac{3}{9}a^6 + \dots = \frac{1}{1 - \epsilon^T/\epsilon_g}. \quad (35)$$

In the simplest case of $\epsilon_g = 1$ and $\Gamma = 0$, Eq. (35) predicts that metal is transparent for both transverse and **L** waves at $\omega > \omega_p$ but both k^L and k^T are complex at $\omega < \omega_p$.

If solid is transparent, a longitudinal wave can be excited under oblique incidence of a p-polarized wave on a plane surface. There are several distinct features of this effect. First, the longitudinal waves can be generated at a flat surface, whereas special efforts should be made to excite the surface plasmon polaritons [4, 5]. Secondly, in the interference pattern, the electromagnetic-field intensity is modulated not along but perpendicular to the interface. Therefore, voids can appear in planes parallel to the surface due to spallation of the solid. According to the definition of ω_p , condition $\omega > \omega_p$ can be met in solids (for example, semiconductors) with a low density of the current carriers. We do not examine this case here because the formula of ϵ^L was derived for degenerate electron gas.

Conclusions

In order to define a spatially dependent dielectric function, all previous researchers considered interaction of matter with a plane electromagnetic wave. This approach is not constructive and rigorous in nano-optics when the field is localized in a cavity and the boundary conditions must be somehow taken into account. We have solved this problem by calculating the response of the medium on an electric field that satisfies the vector Helmholtz equation. The derived spatially dispersive dielectric function depends on the square of the wavenumber, a parameter of the Helmholtz equation, but not the wave vector of a plane wave.

We report the Fresnel reflection coefficients modified due to excitation of the longitudinal waves in metals. Similar generalization was made earlier for the Mie coefficients. Herein, the theory has been verified with simulation of light extinction by nanometer-sized silver and gold clusters. The calculated shift from 3.5 to 3.65 eV and the width of the surface plasmon resonance of the silver particles' beam are in excellent agreement with the experimental data. In addition, the nonlocal model explains the vanishing of the plasmon resonance of golden spheres with diameters of about 2 nm. It is important that **L** wave can be excited on a flat surface by a plane incident wave. This is the main difference of the plasmon polaritons from the surface plasmon polaritons.

The properties of the electromagnetic oscillations in metals have been examined. It has been found that the absolute values of the wavenumbers of the longitudinal waves are much larger than those of the transverse waves. For example, in silver at a photon energy of 3.5 eV, the ratio of the absolute values of the wavenumbers is equal to 130. There, the real part of the wavenumber of the longitudinal wave corresponds to a wavelength of 7 nm. The large difference in the wavenumbers prevents excitation of the **L** waves at a planar surface. However, the **L** modes have been shown to be excited in silver and gold nanometer-sized particles.

Authors' contributions

In this study, the researchers played slightly different roles. VVD derived the longitudinal dielectric function. ORP focused on excitation of the longitudinal modes in various systems with particular attention paid to the LIPSS. Both authors read and approved the final manuscript.

Competing Interests

The authors declare that they have no competing interests.

Publisher's Note

Springer Nature remains neutral with regard to jurisdictional claims in published maps and institutional affiliations.

Received: 30 December 2016 Accepted: 12 July 2017

Published online: 01 August 2017

References

- Bonse J, Höhm S, Kirner SV, Rosenfeld A, Krüger J (2017) Laser-induced periodic surface structures—A scientific evergreen. *IEEE J Sel Top Quantum Electron* 23(3):109–123
- Bonse J, Krüger J, Höhm S, Rosenfeld A (2012) Femtosecond laser-induced periodic surface structure. *J Laser Appl* 24(4):042006
- Bashir S, Rafique MS, Husinsky W (2012) Femtosecond laser-induced subwavelength ripples on Al, Si, CaF₂ and CR-39. *Nucl Instr Meth Phys Res B* 275:1–6
- Novotny L, Hecht B (2006) *Principles of Nano-optics*. Cambridge University Press, New York
- Maier SA (2007) *Plasmonics: Fundamentals and Applications*. Springer, New York
- García de Abajo FJ (2008) Nonlocal effects in the plasmons of strongly interacting nanoparticles, dimers, and waveguides. *J Phys Chem C* 112(46):17983–17987
- Kliwer KL, Fuchs R (1969) Lindhard dielectric functions with a finite electron lifetime. *Phys Rev* 181(2):552–558
- Klimontovich YL, Silin VP (1952) On the spectra of interacting particles, (in Russian). *Zh Ekhsper Teor Fiz* 23:151–160
- Klimontovich YL, Silin VP (1960) The spectra of systems of interacting particles and collective energy losses during passage of charged particles through matter. *Phys.-Uspekhi* 3(1):84–114
- Lifshitz EM, Pitaevskii LP (1997) *Physical Kinetics*. Butterworth–Heinemann, Oxford
- Larkin IA, Stockman MI, Achermann M, Klimov VI (2004) Dipolar emitters at nanoscale proximity of metal surfaces: Giant enhancement of relaxation in microscopic theory. *Phys Rev B* 69(12):121403–1214034
- Lindhard J (1954) On the properties of a gas of charged particles. *Kgl Danske Vidensk Selsk Mat-Fys Medd* 28(8):1–57
- Ordal MA, Bell RJ, Alexander RW Jr, Long LL, Query MR (1985) Optical properties of fourteen metals in the infrared and far infrared: Al, Co, Cu, Au, Fe, Pb, Mo, Ni, Pd, Pt, Ag, Ti, V, and W. *Appl Opt* 24(24):4493–4499
- Datsyuk VV (2011) A generalization of the Mie theory for a sphere with spatially dispersive permittivity. *Ukr J Phys* 56(2):122–129
- Hilger A, Tenfelde M, Kreibitz U (2001) Silver nanoparticles deposited on dielectric surfaces. *Appl Phys B* 73(4):361–372

16. Lynch DW, Hunter WR (1985). In: Palik ED (ed). Handbook of Optical Constants of Solids. Academic Press, San Diego. pp 355–356
17. Bohren CF, Huffman DR (1983) Absorption and Scattering of Light by Small Particles. Wiley, New York
18. Kreibig U, Vollmer M (1995) Optical Properties of Metal Clusters. Springer, Berlin
19. Alvarez MM, Khoury JT, Schaaff TG, Shafigullin MN, Vezmar I, Whetten RL (1997) Optical absorption spectra of nanocrystal gold molecules. *J Phys Chem B* 101(19):3706–3712
20. Johnson PB, Christy RW (1972) Optical constants of the noble metals. *Phys Rev B* 6(12):4370–4379
21. Weber MJ (2002) Handbook of Optical Materials. CRC Press, Boca Raton
22. Hao F, Nordlander P (2007) Efficient dielectric function for FDTD simulation of the optical properties of silver and gold nanoparticles. *Chem Phys Lett* 446(1):115–118
23. Drachev VP, Chettiar UK, Kildishev AV, Yuan HK, Cai W, Shalaev VM (2008) The Ag dielectric function in plasmonic metamaterials. *Opt Express* 16(2):1186–1195

Submit your manuscript to a SpringerOpen[®] journal and benefit from:

- ▶ Convenient online submission
- ▶ Rigorous peer review
- ▶ Open access: articles freely available online
- ▶ High visibility within the field
- ▶ Retaining the copyright to your article

Submit your next manuscript at ▶ springeropen.com
